

doi:10.3788/gzxb20124107.0786

## Second Harmonic Generation with Broadened Band Width in One-dimensional Nonlinear Photonic Crystal at the Oblique Incidence of Light

WANG Ai-hua, ZHAO Jing

(Center of Theoretical Physics, Department of Physics, Capital Normal University, Beijing 100048, China)

**Abstract:** The one-dimensional nonlinear photonic crystals containing defects that are embedded in air are investigated. However, attributed that the reflective second harmonic wave is so strong that it can not be ignored, the slowly varying amplitude approximation is not applicable to such a system. The paper presents a general solution of second harmonic generation without adopting the slowly varying approximation when the incident light is obliquely launched upon the one-dimensional inhomogeneous systems. The result shows that the wavelenghtes corresponding to the defect modes shift to the short-wavelength with the increasing angle of incidence. The broadened band width second harmonic generation with high conversion efficiency can be achieved by modulating the angle of incidence of fundamental wave. Furthermore, this method can be applicable to any one-dimensional inhomogeneous systems and the conversion efficiency of second harmonic generation can be easily and conveniently calculated.

**Key words:** Second Harmonic Generation(SHG); Quasi-phase-matching; Conversion efficiency; Band width

CLCN: O437

Document Code: A

Article ID:1004-4213(2012)07-0786-4

### 0 Introduction

All-optical wavelength conversion is a promising technique in the future wavelength division multiplexing networks. In order to enhance the conversion efficiency, the phase-matching (PM) conditions by using birefringent crystals for the nonlinear process such as second harmonic generation (SHG) are required<sup>[1-4]</sup>. However it leads to a large restriction to the choice of natural nonlinear materials. This problem can be solved by using periodically modulated materials. This mechanism is called quasi-phase-matching (QPM)<sup>[5-6]</sup>, in which the sample with a periodical modulation of the nonlinear optical coefficients can realize the compensation of phase-mismatch between the interacting light waves. Various micro-structures such as periodic optical superlattice (POS), quasi-POS (QPOS), and aperiodic optical superlattice (AOS) have been proposed and extensively investigated theoretically and experimentally<sup>[7-9]</sup>. Recently, broadening single or multiple wavelength SHG can be achieved in AOS sample, which can provide plenty of reciprocal vectors to compensate for the wave vector mismatch<sup>[10-11]</sup>.

Nonlinear photonic crystal (PC) cavities have

attracted widespread interests in recent years because of their ability to enhance SHG. It has been pointed out that the enhancement comes from the defect mode characterized by high EM mode density of states and low group velocity. Some amount of researches on the nonlinearly defective PCs have appeared in the literatures<sup>[12-15]</sup>. Numerical simulations show a giant enhancement of SHG. An experiment of the great enhancement of SHG in a nonlinear optical polymer by strongly confining the fundamental light in a planar micro-cavity has been reported<sup>[16]</sup>. However, most of the work has involved normal incidence, and a wide variety of nonlinear interaction with oblique incident fundament wave (FW) is not well investigated.

Motivated by the above-mentioned works, in this letter, we present a quantitative study of SHG with oblique incidence of the FW in one-dimensional (1D) nonlinear PC embedded in air. Attributed that the reflective second harmonic wave (SHW) is so strong that it can not be ignored, the slowly varying amplitude approximation is not applicable to such a system<sup>[17]</sup>. A general solution of SHG without adopting the slowly varying amplitude approximation is given when light is incident

**Foundation item:** The National Natural Science Foundation of China (No. 11004139), the Natural Science Foundation of Beijing (No. 1102012), and PHR (IHLB) from Beijing

**First author:** WANG Ai-hua(1965—), female, Ph. D. degree, mainly focuses on condensed matter physics. Email: aihua.wang@yahoo.com.cn

**Corresponding author:** ZHAO Jing (1987—), female, M. S. degree, mainly focuses on nonlinear optics. Email: moonzj19871007@126.com

**Received date:** 2011-10-18 **Revised date:** 2012-04-05

obliquely upon 1D inhomogeneous systems. The high conversion efficiency SHGs for various incident angles of FW can be obtained. Furthermore, the method we proposed are applicable to any one-dimensional inhomogeneous systems and the conversion efficiency of SHG can be easily and conveniently calculated.

## 1 Theory

### 1.1 FW and SHW

The typical sample studied is composed of alternatively stacked dielectric-dielectric layers with different refractive indices. We assume that interface of layers is lied on the  $yz$  plane.

The incident light with  $\omega_1 = \omega$  is obliquely launched upon the surface of sample. In a direct non-depleted pump wave approximation, for the  $l$ th layer, the electric field  $E_l^{(1\omega)}(x, y)$  ( $E_l^{(2\omega)}(x, y)$ ) of the FW (the second harmonic wave (SHW)) satisfies the following equations

$$\left(\frac{d^2}{dx^2} + \frac{d^2}{dy^2} + \frac{d^2}{dz^2}\right)E_l^{(1\omega)}(x, y) = 0 \quad (1)$$

$$\left(\frac{d^2}{dx^2} + \frac{d^2}{dy^2} + k_l^{(2\omega)}\right)E_l^{(2\omega)}(x, y) = -k_{20}^2 \chi_l E_l^{(1\omega)^2}(x, y) \quad (2)$$

here  $k_{10} = \omega/c$  ( $k_{20} = 2\omega/c$ ) and  $k_l^{(1)} = n_l^{(1)}k_{10}$  ( $k_l^{(2)} = n_l^{(2)}k_{20}$ ).  $c$  is the light speed in vacuum,  $n_l^{(1)}$  ( $n_l^{(2)}$ ) is the refractive index of the  $l$ th layer material at the FW (SHW) frequency.  $\chi_l$  is nonlinear optical coefficient of the  $l$ th layer.

After giving the formal solution of FW with  $E_l^{(1\omega)}(x, y) = E_l^{(1)}(x) e^{ik_{ly}^{(1)}}$ , we then substitute it into Eq. (1), thus Eq. (1) can be converted into the following equation

$$\left[\frac{d^2}{dx^2} + k_{lx}^{(1\omega)}\right]E_l^{(1\omega)}(x) = 0 \quad (3)$$

where  $k_{lx}^{(1\omega)} + k_{ly}^{(1\omega)} = k_l^{(1\omega)}$

Similarly, for the SHW electric field, we assume  $E_l^{(2\omega)}(x, y) = E_l^{(2)}(x) e^{ik_{ly}^{(2)}}$ , then  $E_l^{(2)}(x)$  meets the following equation

$$\left[\frac{d^2}{dx^2} + k_{lx}^{(2\omega)}\right]E_l^{(2)}(x) = -k_{20}^2 \chi_l E_l^{(1\omega)^2}(x) \quad (4)$$

with  $k_{lx}^{(2\omega)} + k_{ly}^{(2\omega)} = k_l^{(2\omega)}$ , where  $k_{ly}^{(2)} = 2k_{ly}^{(1)}$ . By solving Eq. (3) and (4), we will seek out the solution of SHW. Now, we set

$$E_l^{(1)}(x) = A_l^{(1)} e^{ik_l^{(1)}(x-x_{l-1})} + B_l^{(1)} e^{-ik_l^{(1)}(x-x_{l-1})} \quad (5)$$

and

$$E_l^{(2)}(x) = A_l^{(2)} e^{ik_l^{(2)}(x-x_{l-1})} + B_l^{(2)} e^{-ik_l^{(2)}(x-x_{l-1})} + C_l^+ e^{i2k_l^{(1)}(x-x_{l-1})} + C_l^- e^{-i2k_l^{(1)}(x-x_{l-1})} - \frac{2k_{20}^2 \chi_l A_l^{(1)} B_l^{(1)}}{k_l^{(2\omega)^2}} \quad (6)$$

where  $x_1$  sets 0,  $x_l = x_{l-1} + d_l$  ( $l = 2, 3, \dots$ ),  $d_l$  is the thickness of the  $l$ th layer.  $A_l^{(1)}$  ( $A_l^{(2)}$ ) and  $B_l^{(1)}$  ( $B_l^{(2)}$ ) respectively represent the amplitudes of the “forward” and “backward” FW (SHW) waves

at interface. Substituting Eqs. (5) and (6) into Eq. (4), we have

$$C_l^+ = \frac{-k_{20}^2 \chi_l A_l^{(1)2}}{k_l^{(2\omega)^2} - 4k_l^{(1)2}}$$

$$C_l^- = \frac{-k_{20}^2 \chi_l B_l^{(1)2}}{k_l^{(2\omega)^2} - 4k_l^{(1)2}} \quad (7)$$

### 1.2 Conversion efficiency

Using the formal solution of the FW and SHW, as shown in Eq. (5) and (6), By the continuity of the EM fields at interfaces, we can derive a transfer matrix which establishes a connection between the field amplitudes of the  $(l+1)$  th layer and those of the  $l$ th layer for FW (SHW), the overall transfer matrix is the product of the individual transfer matrix of each layer in sequence. The transfer matrix crucially depends on the sample structure and the FW (SHW) frequency or the dispersion relation. Finally, we can calculate the conversion efficiencies of the “forward” and “backward” SHGs, which are denoted by  $\eta_{\text{forth}}$  and  $\eta_{\text{back}}$ , respectively. Considering the initial condition  $A_1^{(2)} = 0$  and  $B_n^{(2)} = 0$ , the conversion efficiencies of the “forward” and “backward” waves are evaluated respectively by

$$\eta_{\text{forth}} = \frac{n_N^{(2)} |A_N^{(2)}(x_{N-1})|^2}{n_1^{(1)} |A_1^{(1)}|^2} \quad (8a)$$

and

$$\eta_{\text{back}} = \frac{n_1^{(1)} |B_1^{(2)}(x_1)|^2}{n_1^{(2)} |A_1^{(1)}|^2} \quad (8b)$$

where  $N$  denotes the total number of layers in sample.

## 2 Calculation

We now consider a sample consisting of alternating stacked dielectric-air-nonlinear material layers. We denote the structural configuration as  $(AB)_m C (AB)_m$ . Layers A, B, and C possess different refractive indices. Layers  $(AB)_m$  can be regarded as Bloch mirrors for the FW and C as nonlinear material defect layer, and the whole sample can be equivalent to a F-P cavity. We choose  $m = 10$  in calculation and assume that layer A(B) is made by BaTiO<sub>3</sub> (air) material. The refractive index and thickness of layer A(B) are  $n_A = 2.4$  ( $n_B = 1$ ) and  $d_A = 0.34 \mu\text{m}$ , ( $d_B = 0.26 \mu\text{m}$ ), respectively. Layer C is chosen as the LiNbO<sub>3</sub> crystal with a thickness of  $d_C = 1.00 \mu\text{m}$ . Its refractive index is referred to [18] and its nonlinear coefficient  $d_{33}$  is 47.0 pm/V, referred to Ref. [19]. The intensity of the incident FW wave sets  $I = 1.328 \times 10^9 \text{ W/m}^2$ , corresponding to  $|E_1^{(1)}(x_1)|^2 = 1.00 \text{ V}^2/\mu\text{m}^2$ .

We calculate the transmission spectrum of the above-mentioned configuration for two different angle of incidence  $\theta$ , (a) for  $\theta = 0$ , and (b) for  $\theta = 20^\circ$ , as shown in Fig. 1. It is clearly from Fig. 1(a)

that there exists photonic band gaps (PBGs) over the range from  $0.948 \mu\text{m}$  to  $1.245 \mu\text{m}$ , there are two strong peaks appearing within the PBG and the corresponding defect modes are  $1.003 \mu\text{m}$  (denoted as DMI) and  $1.164 \mu\text{m}$  (denoted as DMII). We investigate the transmission spectrum for other angles of incidence, and we find that the general picture of transmission spectrum does not change, but the entire spectrum moves towards shorter wavelength. For example, for the angle of arrival with  $\theta=20^\circ$ , the range of PBG is from  $0.927 \mu\text{m}$  to  $1.229 \mu\text{m}$ , the two corresponding defect modes are  $0.987 \mu\text{m}$  for DMI and  $1.148 \mu\text{m}$  for DMII.

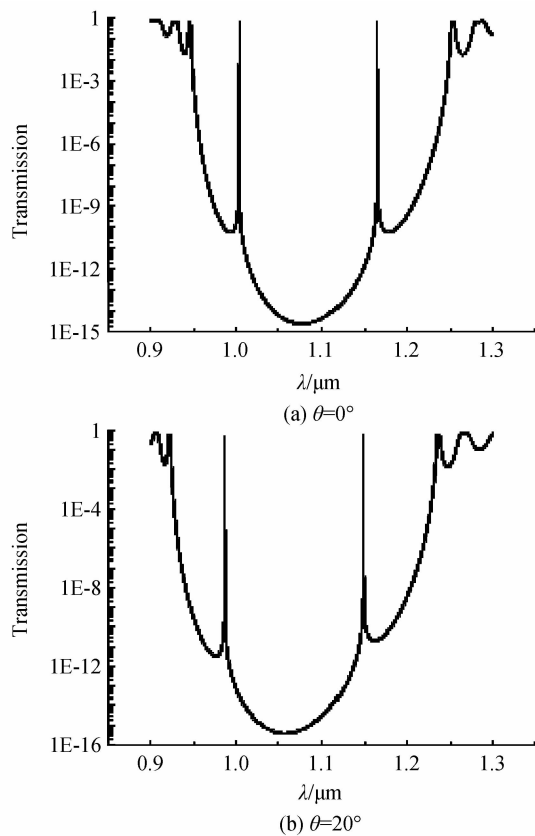


Fig. 1 Transmission spectra for two values of  $\theta$

We describe the variation of wavelenghtes for the defect modes as a function of incident angle  $\theta$  in Fig. 2, (a) for DMI, and (b) for DMII. It is clearly that the wavelenghtes of the defect modes become shorter with the increasing incidence. When  $\theta=0^\circ$ , the DMI is located at  $1.003 \mu\text{m}$ , while for  $\theta=20^\circ$ , it is in the location of  $0.927 \mu\text{m}$  wavelength. Obviously, it moves about  $0.076 \mu\text{m}$  with the changing  $\theta$  from  $0$  to  $20^\circ$ . In the same case, the wavelength of DMII is in the place of  $1.229 \mu\text{m}$  for  $\theta=0^\circ$ , and situates  $1.148 \mu\text{m}$  for  $\theta=20^\circ$ , the corresponding shifting is about  $0.081 \mu\text{m}$ . It is evident that the defect modes can move around a few dozen nanometer within 20-degree angle of incidence. Noting that we mainly discuss the SHG in the case of incidence with small-angle,

considering the FW and SHW propagating in a different direction. In this case, the interaction length of FW and SHW is shortened with the increasing incidence, this induce the debased SHG.

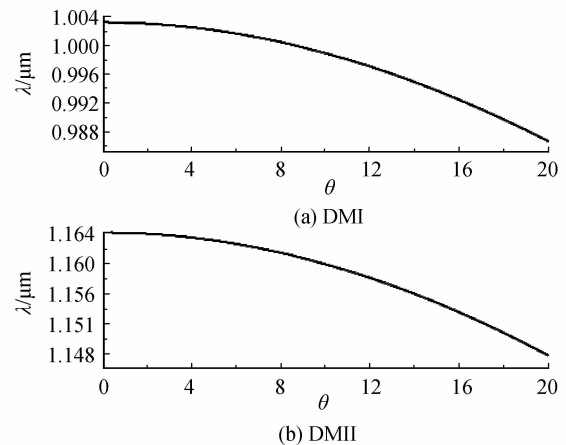


Fig. 2 The variation of wavelenghtes for two modes

Fig. 3 shows the variation of conversion efficiency for DMI and DMII with the incident angle  $\theta$ , (a) for DMI, and (b) for DMII. It is obvious that the conversion efficiency varies in oscillation with the increasing incident angle, and the high conversion efficiency SHG can be achieved in a rather large angle range. For DMI, in the range of  $\theta=13^\circ$ , the SHG with high conversion efficiency oscillates violently, and the highest total conversion efficiency for DMI is 0.28, and the lowest one is 0.007 9. When  $\theta>13^\circ$ , the

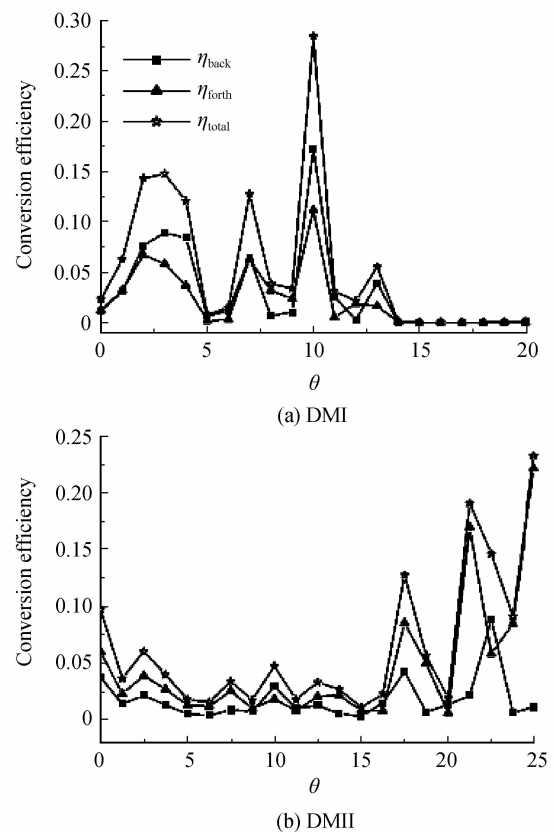


Fig. 3 The variation of conversion efficiency with  $\theta$  for two modes

conversion efficiency is rapidly reduced, as shown in Fig. 3(a). While for DMII, the SHG conversion efficiency is relatively flat changes within 13-degree incidence. The highest conversion efficiency is 0.097 with the angle of incidence  $\theta = 0$ , the corresponding defect mode is  $1.164 \mu\text{m}$ ; when  $\theta = 12^\circ$ , the lowest conversion efficiency is 0.011 for the defect mode  $1.158 \mu\text{m}$ . When  $\theta > 13^\circ$ , the SHG conversion efficiency exhibits a significant change in oscillation, with the highest conversion efficiency 0.23 for  $\theta = 20^\circ$  and the lowest one 0.02 for  $\theta = 16^\circ$ , the corresponding defect modes are  $1.148 \mu\text{m}$  and  $1.154 \mu\text{m}$ , respectively. It is obvious that the high conversion efficient SHG can be achieved in the range of wide-angle. For conventional samples such as QPOS or AOS, QPM should be satisfied simultaneously for multiple wavelengths, this leads to the deduced SHGs. While in our method, the SHG conversion efficiencies are not affected in the case of multiple wavelength.

### 3 Conclusion

In summary, we show a general solution of SHG without using the slowly varying amplitude approximation for 1D inhomogeneous system with oblique incidence. The nonlinear PC containing defects is investigated. We find that the defect modes move towards shorter wavelength with the increasing incident angle, and the high conversion efficient SHG can be obtained in the range of wide-angle.

#### References

- [1] YARIV A, YEH P. Optical wave in crystal[M]. New York: Wiley, 1984.
- [2] SHEN Y R. The principles of nonlinear[M]. New York: Wiley, 1984.
- [3] LIU X, DENG D Q, WU L A, et al. Study of the retracing behavior of the phase-matching angle in second harmonic generation[J]. *Chinese Physics Letters*, 1994, **11**(5): 273-276.
- [4] LU H, XUE C H, JIANG H T, et al. Optical phase conjugation enhancement in one-dimensional nonlinear photonic crystals containing single-negative materials [J]. *JOSA B*, 2011, **28**(4): 856-860.
- [5] BLOEMBERGEN N, SIEVERS A J. Nonlinear optical properties of periodic laminar structures[J]. *Applied Physics Letters*, 1970, **17**(11): 483-486.
- [6] ARMSTRONG A, BLOEMBERGEN N, DUCUING J, et al. Interactions between light waves in a nonlinear dielectric[J]. *Physical Review*, 1962, **127**(6): 1918-1939.
- [7] ZHU S N, ZHU Y Y, MING N B. Quasi-phase-matched third-harmonic generation in a quasi-periodic optical superlattice[J]. *Science*, 1997, **278**(5339): 843-846.
- [8] GU B Y, DONG B Z, ZHANG Y, et al. Enhanced harmonic generation in aperiodic optical superlattices [J]. *Applied Physics Letters*, 1999, **75**(15): 2175.
- [9] ZHAO L M, GU B Y, ZHOU Y S, et al. Second-harmonic generation and multiple mode effects in aperiodic optical superlattices with finite lateral width[J]. *Journal of Physics: Condensed Matter*, 2003, **15**(29): 4889-4902.
- [10] GU X, CHEN X F, CHEN Y P, et al. Narrowband multiple wavelengths filter in aperiodic optical superlattice[J]. *Optics Communications*, 2004, **237**(1): 53-58.
- [11] ZENG X L, CHEN X F, WU F, et al. Second-harmonic generation with broadened flattop bandwidth in aperiodic domain-inverted gratings[J]. *Optics Communications*, 2002, **204**(1-6): 407-411.
- [12] REN F F, LI R, CHENG C, et al. Giant enhancement of second harmonic generation in a finite photonic crystal with a single defect and dual-localized modes[J]. *Physical Review B*, 2004, **70**(24): 245109(4).
- [13] SHI B, JIANG Z M, WANG X. Defective photonic crystals with greatly enhanced second-harmonic generation [J]. *Optics Letters*, 2001, **26**(15): 1194-1196.
- [14] ZHAO L M, GU B Y. Giant enhancement of second harmonic generation in multiple photonic quantum well structures made of nonlinear material[J]. *Applied Physics Letters*, 2006, **88**(12): 122904(3).
- [15] ZHAO L M, GU B Y. Enhanced second-harmonic generation for multiple wavelengths by defect modes in one-dimensional photonic crystals[J]. *Optics Letters*, 2006, **31**(10): 1510-1512.
- [16] CAO H, HALL D B, TORKEKELSON J M, et al. Large enhancement of second harmonic generation in polymer films by microcavities[J]. *Applied Physics Letters*, 2000, **76**(5): 538(3).
- [17] LI Z Y, GU B Y, YANG G Z. Slowly varying amplitude approximation appraised by transfer-matrix approach [J]. *Physical Review B*, 1999, **60**(15): 10644-10647.
- [18] MEYN J P, FEJER M M. Tunable ultraviolet radiation by second-harmonic generation in periodically poled lithium tantalite[J]. *Optics Letters*, 1997, **22**(16): 1214-1216.
- [19] DMITRIYEV V G, GURAZDYAN G G, NIKOGOSYAN D N. Handbook of nonlinear optical crystals [M]. Berlin: Springer, 1997.

## 倾斜入射光入射于一维非线性光子晶体中带宽加宽的二次谐波的产生

王爱华, 赵静

(首都师范大学 物理系 理论物理中心, 北京 100048)

**摘要:**研究了置于空气中的含缺陷的一维非线性光子晶体中二次谐波的产生. 由于反射的二次谐波很强而不能忽略, 缓变振幅近似在系统中是不适用的. 本文提出了一种不采用缓变振幅近似来处理二次谐波产生问题的方法, 并应用这种方法计算相关的二次谐波转换效率. 结果表明: 随着入射波角度的增加, 缺陷模对应的波长将变短, 并且通过调整基频波入射的角度, 可以产生宽带并且高转换效率的二次谐波. 这个方法适用于任何一维非均匀系统, 可以简单方便地计算出二次谐波转换效率.

**关键词:**二次谐波产生; 准位相匹配; 转换效率; 带宽